Ventricular function after operation for transposition of the great arteries with special reference to myocardial deformation

by

Eirik Pettersen

Department of Cardiology
Oslo University Hospital Rikshospitalet

Faculty of Medicine
Faculty Division Rikshospitalet
University of Oslo
Norway

Series of dissertations submitted to the
Faculty of Medicine, University of Oslo
No. 994

ISBN 978-82-8072-515-8

Cover: Inger Sandved Anfinsen.
Printed in Norway: AiT e-dit AS.

Produced in co-operation with Unipub.
The thesis is produced by Unipub merely in connection with the
thesis defence. Kindly direct all inquiries regarding the thesis to the copyright
holder or the unit which grants the doctorate.

Table of contents

Acknowledgements

The present work was carried out at the Department of Cardiology, Rikshospitalet University Hospital, between 2003 and 2007 and funded by a research fellowship from the Norwegian Research Council (September 2003-August 2006), the University of Oslo (September 2006-February 2007) and Rikshospitalet University Hospital (March 2007-August 2007). In addition, I have received grants from Dr. Alexander Malthes legat and the Norwegian Society of Cardiology, for which I am grateful.

Professor Halfdan Ihlen was my principal advisor during the first half of my period as a research fellow. It was a great privilege for me to have as my mentor someone who has played a central role in the development of echocardiographic techniques. Always available and interested both professionally and personally, his support and guidance have been of the greatest importance to my work.

Kai Andersen took on the role as principal advisor when Halfdan Ihlen retired. Always encouraging and positive, he introduced me to the field of congenital heart disease and taught me the importance of a structured approach and rigorous scientific standards, to which I can only hope to aspire. I consider myself very fortunate to have benefited from his experience and I greatly value our friendship.

As my second advisor, I am grateful to have had Professor Otto Smiseth, one of the most distinguished scientists in his field. He has given invaluable input at all stages of the process, and I remain in awe of his ability to extract the essence of research findings and formulate them succinctly.

Professor Thor Edvardsen, Professor Hans-Jørgen Smith and Bjarne Smevik have provided expert assistance with the MRI recordings and analyses. Professor Erik Thaulow, enthusiastic and inspiring, has been a valuable discussion partner. Per Morten Fredriksen has afforded great help with the exercise testing. I am also indebted to Professor Harald Lindberg for providing the patient material without which this thesis would not have been possible.

To my colleagues Stig Urheim, Thomas Helle-Valle, Trond Vartdal, Anders Opdahl, Ola Gjesdal, Espen Remme and Ketil Lunde – thank you for your help, advice and support.

Svend Aakhus and the staff at the echocardiographic laboratory at Rikshospitalet, Pia Bryde, Joke Andreassen and Richard Massey, also deserve special mention. Pia Bryde has

instilled in me the importance of a systematic echocardiographic examination, from which I profit daily and probably will for the rest of my career.

I thank my parents, who have provided generous support in all ways possible. And finally, Arnold, my husband and daily reminder that the echocardiogram does not tell the entire truth about the heart – I thank you.

List of papers

1. Pettersen E, Helle-Valle T, Edvardsen T, Lindberg H, Smith HJ, Smevik B, Smiseth OA, Andersen K. Contraction Pattern of the Systemic Right Ventricle - Shift from Longitudinal to Circumferential Shortening and Absent Global Ventricular Torsion. J Am Coll Cardiol. 2007; 49:2450-6.

2. Pettersen E, Lindberg H, Smith HJ, Smevik B, Edvardsen T, Smiseth OA, Andersen K. Left Ventricular Function in Patients with Transposition of the Great Arteries Operated with Atrial Switch. Pediatr Cardiol. 2008; 29:597-603.

3. Pettersen E, Fredriksen PM, Urheim S, Thaulow E, Smith HJ, Smevik B, Smiseth OA, Andersen K. Ventricular Function in Patients with Transposition of the Great Arteries Operated with Arterial Switch. Am J Cardiol. 2009; 104:583-9.

List of abbreviations

EF	ejection fraction
IVS	interventricular septum
LV	left ventricle
MRI	magnetic resonance imaging
RV	right ventricle
SD	standard deviation
STE	speckle tracking echocardiography
TDI	tissue Doppler imaging
TGA	transposition of the great arteries

Introduction

Background

Transposition of the great arteries (TGA) is the second most common cyanotic congenital heart defect. With advances in surgical treatment, more patients survive into adulthood and constitute a growing patient population. Evaluation of ventricular function is an integral part of the follow-up of TGA patients. Furthermore, the available treatment strategies for TGA not only reflect evolving surgical techniques but also offer a unique possibility for studying ventricular physiology under different loading conditions. Advances in imaging techniques, especially echocardiography and magnetic resonance imaging (MRI), permit quantification not only of global ventricular function, but also assessment of regional myocardial function, which might add useful information when evaluating this patient group.

Transposition of the great arteries

Transposition of the great arteries is characterized by anomalous ventriculo-arterial connections. There are two forms, D-transposition, the subject of this thesis, and L-transposition or congenitally corrected transposition. L-transposition is described by discordant atrioventricular and ventriculo-arterial connections and will not be discussed further here.

D-transposition of the great arteries (henceforth referred to simply as transposition or TGA) represents 5-7 % of congenital heart disease and is the second most common cyanotic defect after tetralogy of Fallot (1). It affects primarily males, with a male:female ratio of 2:1. The morphology is described by atrioventricular concordance and ventriculo-arterial discordance, i.e. while the atria and ventricles are connected in the normal arrangement, the anatomic right ventricle (RV) connects to the aorta and the anatomic left ventricle (LV) to the pulmonary artery (Figure 1). Furthermore, the aorta is located anteriorly and to the right and the great arteries run in parallel instead of in their normal, almost perpendicular relation. The result is two separate, parallel circulations rather than a systemic and pulmonary circulation connected in series: De-oxygenated blood from the systemic circulation enters the right atrium and continues through the RV into the aorta, while oxygenated blood returning from

the pulmonary circulation to the left side of the heart is pumped back into the pulmonary circulation.

Transposition is often associated with other cardiac defects, the most common being ventricular and/or atrial septal defect, patent ductus arteriosus and LV outflow tract obstruction, as well as coarctation of the aorta, pulmonary stenosis, atrioventricular valve atresia and ventricular hypoplasia.

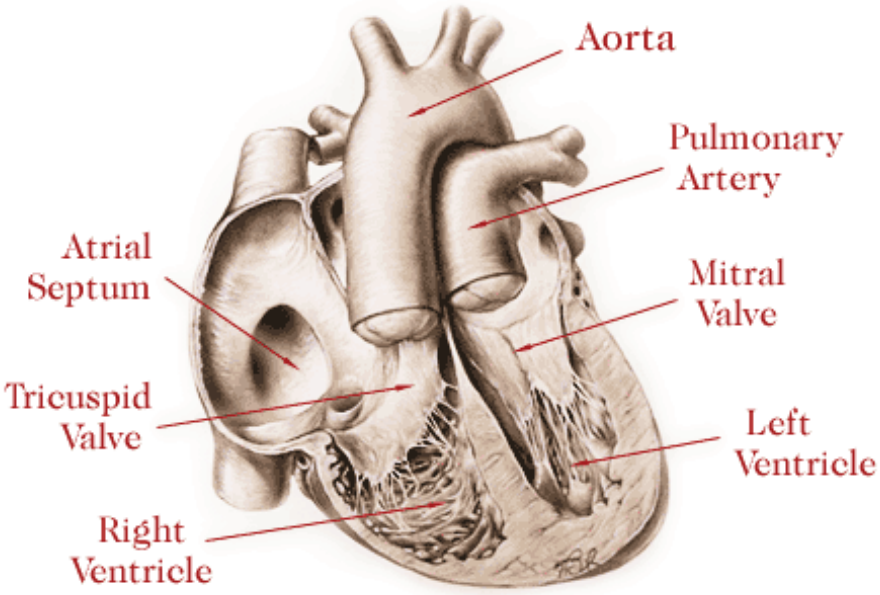

Figure 1

Transposition of the great arteries. The aorta is connected to the right ventricle, the pulmonary artery to the left ventricle. The aorta is located anteriorly and to the right, and the great arteries run in parallel instead of in their normal perpendicular relation. Illustration by Ted Bloodheart, reproduced with permission from The Children's Hospital Los Angeles.

After birth, the connections between the left and right sides of the circulation, both physiological (foramen ovale and ductus arteriosus) and pathological (atrial or ventricular septal defect), ensure that oxygenated blood enters the systemic circulation. When the physiological connections close cyanosis ensues, depending on the size of the atrial or ventricular septal defect, if present. Palliation may be obtained by balloon atrial septostomy (Rashkind procedure) and pharmacological treatment to keep the ductus arteriosus open. However, definite treatment is surgery, with the two main approaches being the atrial and the arterial switch procedures.

Surgical treatment

The atrial switch procedure was introduced in 1959 by Senning (2). The Senning-operation is a physiological correction and consists of a reconstruction of the atrial septum to create a baffle that diverts systemic venous return from the right to the left atrium and pulmonary venous return from the left to the right atrium (Figure 2). The RV then remains the systemic ventricle. Mustard modified this procedure in 1964 (3), creating the atrial baffle from pericardial tissue. Subsequently, synthetic material was used for the baffle. Late complications are primarily arrhythmias due to atrial scarring, RV failure, tricuspid regurgitation and baffle obstruction or leak (1, 4, 5). Ten-year survival is approximately 90% for patients without associated lesions, while 20-year survival is about 80% (6, 7).

The arterial switch procedure was first performed in 1975 by Jatene (8) and modified by Lecompte in 1981 (9). It is an anatomical correction where the great arteries are transected and switched to their normal position. The coronary arteries are excised from the native aortic root, which becomes the neo-pulmonary root, and re-implanted in the neo-aortic root (the native pulmonary root) (Figure 3). This restores the LV as the systemic ventricle. Recognized complications are ostial coronary artery stenoses, supravalvular pulmonary artery stenosis and aortic regurgitation (10-12). Long-term follow-up data are lacking due to this being a relatively new procedure, but data at 10 years show around 90% survival, remaining the same at 15 years follow-up (13, 14).

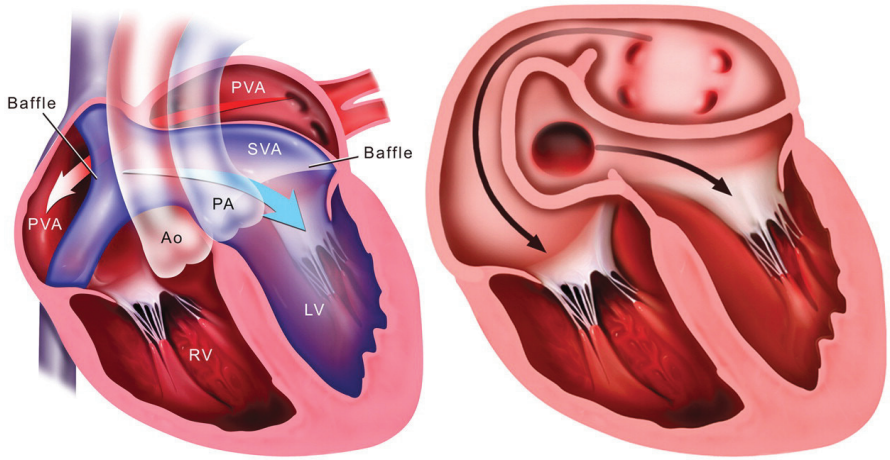

Figure 2

Atrial switch in the manner described by Senning. The interatrial septum is incised and reconstructed to create a baffle that directs blood from the pulmonary venous atrium (PVA) over to the right side of the heart and into the right ventricle (RV), and from the systemic venous atrium (SVA) into the left ventricle (LV). Ao, aorta; PA, pulmonary artery. Illustration from *Gaca et al. Repair of congenital heart disease: a primer – part 1. Radiology 2008;247:617-63*. Reproduced with permission from Dr Ana Maria Gaca and the Radiological Society of North America.

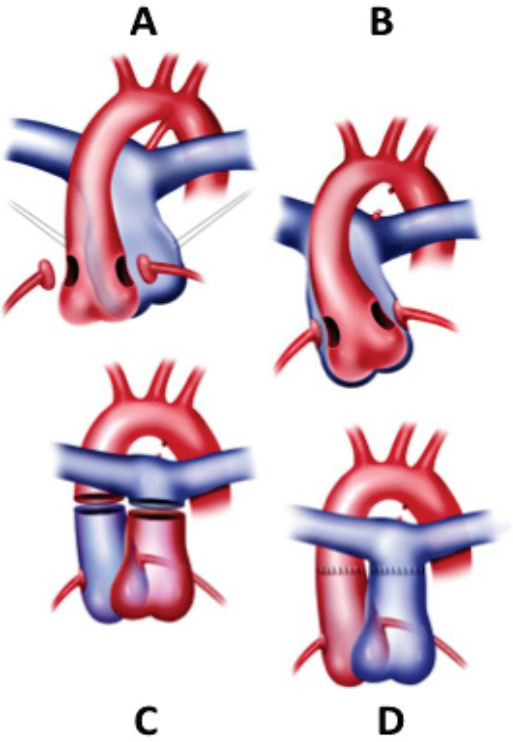

Figure 3

Arterial switch. The coronary arteries are excised (A) and implanted (B) in the neo-aortic (native pulmonary) root. The great arteries are transected, the pulmonary artery shifted forward (C) and sutured to the neo-pulmonary (native aortic) root, while the aorta is sutured to the neo-aortic root (D). Illustration from *Gaca et al. Repair of congenital heart disease: a primer – part 1. Radiology 2008;247:617-63*. Reproduced with permission from Dr Ana Maria Gaca and the Radiological Society of North America.

Ventricular function

Assessment of ventricular function is essential in the follow-up of operated TGA patients. However, this poses a challenge in TGA subjects for several reasons. Traditionally, ventricular function has been evaluated in terms of global function. However, measures of global function such as ejection fraction (EF) may be normal despite changes in regional function and incipient myocardial function may be overlooked. Additionally, there might be changes in contraction pattern related to gross architectural differences between normal hearts and TGA hearts, confounding the assessment of ventricular function. Furthermore, in atrial switch-operated patients, the altered loading conditions might influence the contraction pattern, which does not necessarily represent myocardial dysfunction. For instance, reduced longitudinal function has been reported in atrial switch-operated patients and interpreted as reduced ventricular function (15, 16). However, longitudinal shortening represents only one aspect of myocardial deformation, and possible adaptive changes in other dimensions should be defined before ventricular dysfunction can be established.

Contraction of myocardial fibres causes both longitudinal and circumferential shortening, as well as resultant radial thickening. In addition, contraction of fibres arranged obliquely to the ventricular long axis gives rise to ventricular torsion or twist. These elements of myocardial deformation all contribute to ventricular ejection and may be affected to various degrees in cardiac disease. In summary, myocardial function should ideally be assessed not only globally, but also on a regional level and in several dimensions.

Myocardial deformation may be assessed non-invasively by echocardiography or MRI. Both techniques permit quantification of regional myocardial deformation: Echocardiography through the modalities of tissue Doppler imaging (TDI) and the more recently commercially available speckle tracking echocardiography (STE); MRI through MRI tagging. Using these techniques, the movement and deformation of a myocardial segment can be measured throughout the cardiac cycle.

Aims of the thesis

The general aim of this thesis was to describe ventricular function in TGA patients operated with atrial or arterial switch, with special emphasis on myocardial deformation assessed in terms of longitudinal and circumferential contraction and ventricular torsion.

Specific aims:

1. From a physiological perspective, our interest was to study myocardial deformation in TGA patients operated with atrial switch where loading conditions are altered (Papers 1 and 2), and arterial switch where the ventricles are returned to their normal roles (Paper 3). Integrating these findings, we wished to investigate the relative contributions of loading conditions versus possible inherent structural alterations to ventricular contraction pattern.
2. Of clinical relevance, possible adaptive changes in contraction pattern due to altered loading conditions should be defined before evidence of ventricular dysfunction can be established (Paper 1). Furthermore, we sought to determine if there were signs of incipient or manifest myocardial dysfunction at mid- to long-term follow-up after operation for TGA (Papers 1, 2 and 3).
3. From a methodological viewpoint, we wished to investigate whether myocardial deformation variables might provide useful information in the study and follow-up of TGA patients (Papers 1, 2 and 3).

Material

Paper 1 and 2

Senning-operated TGA patients. Eighteen Senning-operated TGA patients (6 women) aged 18.4±0.9 years were identified from the hospital's database. One patient died suddenly before the planned examination. Three patients were excluded from analyses: Two because of hemodynamically significant lesions, the third because of poor quality MRI recordings. Thus 14 patients were included.

Healthy controls. Fourteen healthy volunteers (4 women) aged 27.4±1.2 years served as controls.

Operated controls. To exclude that the findings in the Senning-operated patients might merely reflect post-operative effects, we studied 14 patients (3 women) aged 18.1±4.8 years successfully operated for congenital heart disease but with a systemic LV (3 for aortic valvular disease, 5 for perimembranous ventricular septal defects, 6 for TGA with arterial switch).

Paper 3

TGA patients operated with arterial switch. Twenty-two patients (7 females) with simple TGA aged 12.4±2.3 years operated as infants with one-stage arterial switch were identified from the hospital's database. We selected the oldest patients and excluded patients with complex or known residual lesions or psychomotoric disability.

Healthy controls. Twenty-two healthy volunteers (8 females) aged 12.7±2.3 years served as controls.

Methods

Clinical examination

All patients underwent clinical examination, including recording of blood pressure and ECG.

Exercise testing

Paper 1 and 2

All patients performed bicycle exercise testing with an initial work load of 25 or 50 W, individualized to yield an exercise duration of about 10 minutes, increased by 25 W every 2 minutes. Ventilatory oxygen uptake (Vo_2) was measured with an open circuit-technique (EOS/SPRINT, E. Jaeger, Wurzburg, Germany).

Paper 3

All patients performed treadmill exercise testing using the Oslo protocol (17). The tests were conducted to volitional fatigue on a motor-driven treadmill (Technogym, Italy). Ventilatory oxygen uptake and spirometry were assessed by SensorMedics Vmax29 (Yorba Linda, California, USA).

.

Standard echocardiographic examination

Recordings were obtained with a GE Vingmed Vivid 7 scanner (GE Vingmed Ultrasound, Horten, Norway). All patients underwent a standard echocardiographic examination, including measurements of ventricular dimensions and assessment of valvular function. We also evaluated the operation result and potential complications such as baffle leak or obstruction in the Senning-operated patients and pulmonary artery stenosis, aortic root dilatation or aortic regurgitation in the arterial switch-operated patients.

Assessment of global ventricular function

Global ventricular function was assessed by MRI. MRI scans were performed using a 1.5 T scanner (Magnetom Vision Plus, Siemens, Erlangen, Germany). Ventricular mass, volumes and EF were calculated from area measurements of multiple short axis breath-hold images covering the entire ventricle (18). In paper 3, LV volumes and EF were also assessed by echocardiography.

Assessment of ventricular geometry

Ventricular geometry was described by the position of the interventricular septum (IVS) as the ratio between the end-systolic septum to free-wall internal diameters of the two ventricles. In paper 1 and 2, we also measured free wall radius of curvature using a dedicated Matlab application (MathWorks Inc., Natick, MA, USA) (Figure 4).

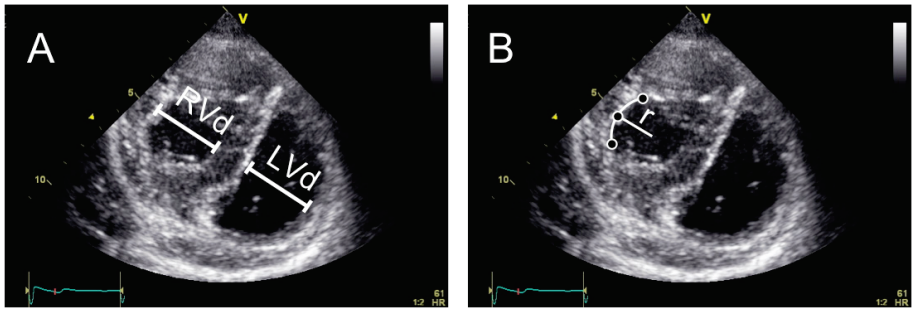

Figure 4

Echocardiographic short-axis section of the heart in a Senning-operated patient schematically illustrating measurement of right and left ventricular diameters (RVd and LVd) in panel A and radius of curvature (r) in panel B. Notice the near circular shape of the systemic right ventricle and the reversal of the septal curvature compared to a normal heart.

Assessment of myocardial deformation

Myocardial deformation was assessed in terms of longitudinal and circumferential shortening as well as ventricular torsion. In evaluating myocardial deformation, two echocardiographic techniques – TDI (paper 1 and 2) and STE (paper 3) – and MRI tagging were used.

Tissue Doppler imaging

Tissue Doppler imaging is based on the measurement of tissue velocities utilizing the Doppler principle. While moving blood reflects low amplitude and high velocity Doppler signals, the myocardium generates signals of high amplitude and low velocity. Therefore tissue velocities can be captured by reducing the threshold of the velocity filter (to detect the low tissue velocities) and lowering the gain amplification (to eliminate the low amplitude blood flow signals). A sample volume, or region of interest, may be placed in the myocardium and regional tissue velocity can then be measured. The velocity obtained represents the component of motion of a given segment in the direction parallel to the ultrasound beam. Velocity measurement is thus angle dependent. It is also sensitive to frame rate, and a low frame rate may cause an underestimation of peak values. A further limitation is that the velocity of one myocardial segment is dependent on function in neighbouring segments (tethering effect) and is affected by cardiac translation (movement of the entire heart within the thorax). Consequently, tissue velocity does not represent true regional function, but is rather the resultant velocity vector along the axis of the ultrasound beam.

In order to quantify true regional function, the techniques of strain rate and strain measurement were introduced (19, 20). The Lagrangian strain ε of an object is the change in object length ($L-L_0$) relative to its unstressed length (L_0):

$$\varepsilon=(L-L_0)/L_0$$

By definition then, negative values represent shortening or compression of the object – in this case a myocardial segment - and positive values represent lengthening. Derivation of ε yields strain rate, i.e. the rate of deformation of the segment. However, when utilizing TDI, segment length is not measured directly but deformation is calculated from instantaneous velocities. Using a sample volume with a fixed offset distance (Δx), a velocity difference across this distance ($v(x)-v(x+\Delta x)$) is calculated. When dividing the velocity difference by the distance

of the offset distance, we obtain the instantaneous velocity gradient or natural, as opposed to Lagrangian, strain rate:

$$SR=(v(x)-v(x+\Delta x))/\Delta x$$

By integrating strain rate over time, natural strain is obtained. The method has been validated against both sonomicrometry (20) and MRI (21). As can be seen from the equation, calculation of strain rate depends on measurement of velocities along the ultrasound beam. Assuming that tethering and translation equally affects the points between which the velocity gradient is measured, these movements should not significantly affect strain and strain rate. However, these measures are still angle dependent (20, 22).

Speckle tracking echocardiography

Speckle tracking echocardiography is a technique aiming to overcome the angle dependency of tissue Doppler imaging. It is based on tracking the movement of speckles, myocardial acoustic markers (23). The speckles in the grey scale image are the result of the interference pattern generated from the ultrasound beams. This pattern follows the movement of the myocardium and remains relatively stable, and can be tracked from frame to frame. From this tracking, the deformation of the myocardium throughout the cardiac cycle can be calculated and data for velocities, strain rate and strain can be extracted. In this case, Lagrangian strain is measured. The method has been validated against both sonomicrometry (24) and MRI tagging (25).

Rotation can also be assessed; the ventricular centre of gravity is determined and a region's rotation relative to this centre is calculated (26). Although the speckle pattern of a region is relatively stable, it is affected by out-of-plane motion and small changes in the interference pattern over time. Therefore, if frame rate becomes too low, the speckle pattern may have changed sufficiently from one frame to the next for tracking to become inaccurate.

Magnetic resonance imaging tagging

Tags are patterns of demagnetization superimposed on tissue. When the tissue is deformed, the tag lines will be deformed correspondingly. The deformation of the tag lines relative to one another can then be used to calculate tissue deformation (27, 28). In our study, the myocardium was tagged at end-diastole and deformation followed through systole.

Striped tags were prescribed separately in two orthogonal orientations (45° and 135°) using spatial modulation of magnetization in a grid pattern with 8 mm distance between tags (Figure 5). Time resolution was 35 milliseconds. Images were acquired at breath holds and triggered by ECG. Recordings were analyzed by Harmonic Phase Imaging (HARP, version 1.0, Diagnosoft Inc. Palo Alto, CA) (29).

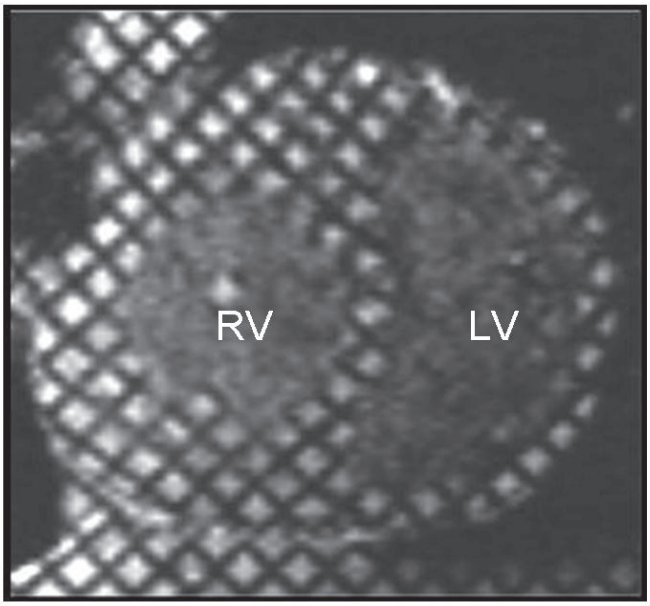

Figure 5

Short-axis magnetic resonance image of the systemic right ventricle (RV) and subpulmonary left ventricle (LV) in a Senning-operated patient illustrating tagging lines. The deformation of the myocardium can be measured throughout systole through movement of the tagging lines relative to one another.

Myocardial deformation assessment in papers 1 and 2

Measurement of myocardial shortening. Myocardial shortening was evaluated by measuring strain and strain rate using TDI. Color TDI images (frame rate 90-240 frames per second) of both ventricles were obtained and analyzed off-line using dedicated software (EchoPac, GE Vingmed Ultrasound, Horten, Norway) by an observer blinded to the MRI data. Regional myocardial function was assessed by peak systolic strain and strain rate. End-diastole was defined at the peak R of the electrocardiographic QRS-complex, end-systole as the first negative cross-over of the velocity curve. Longitudinal regional function was measured in the apical, mid and basal segment of the free wall of both ventricles as well as in the IVS using a sample volume of 6 mm (Figure 6). Circumferential regional function was measured in the RV and LV free wall at the mid-ventricular level. All measurements were averaged over three cardiac cycles. To validate measurements of circumferential strain, tagged MRI images were analyzed by Harmonic Phase Imaging (HARP, version 1.0, Diagnosoft Inc. Palo Alto, CA). Circumferential peak systolic strain at the mid-ventricular level of the RV lateral wall was measured as a reference method for Doppler-derived circumferential strain.

Ventricular torsion. Basal and apical systolic global rotation, i.e. rotation of the entire short-axis slice, were measured from tagged MRI images using HARP. Ventricular torsion was calculated as the difference between basal and apical rotation. Global rotation could not be calculated for the normal RV, as the rotation algorithm presupposes a relatively circular short-axis shape. However, rotation of the entire heart could be measured using the common center of gravity of the two ventricles as a reference point, allowing extraction of regional data for rotation of the free walls of the normal RV and subpulmonary LV.

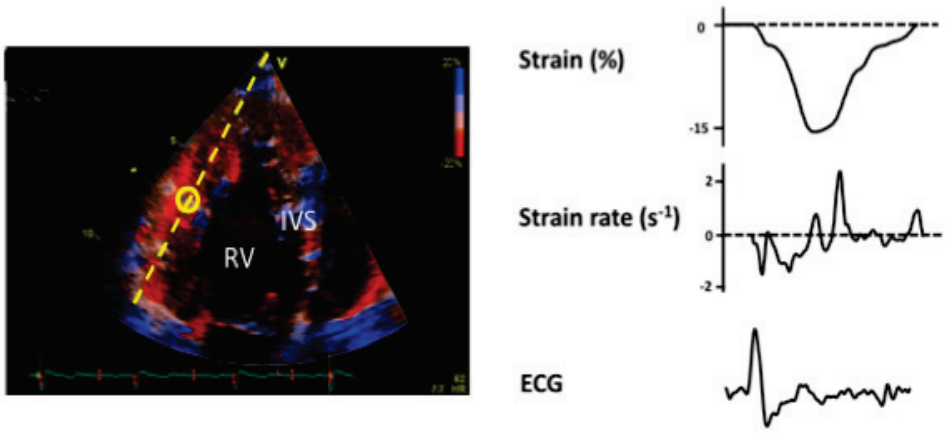

Figure 6

Tissue Doppler imaging. In the left hand panel is a color-coded tissue Doppler image of the systemic right ventricle (RV) in the apical four-chamber view; the yellow line illustrates the direction of the ultrasound beam and the yellow circle represents a sample volume placed in the mid segment of the free wall. In the right hand panel are the derived strain and strain rate curves. Sample volumes were placed in the apical, mid and basal segments of the ventricular free walls and the interventricular septum (IVS) for measurement of longitudinal function, as well as in the mid segment of the ventricular free wall in the short-axis section for measurement of circumferential function.

Myocardial deformation assessment in paper 3

Gray scale images (frame rate 69-112 frames per second) were analyzed off-line using dedicated software (EchoPac, GE Vingmed Ultrasound, Horten, Norway). Regional myocardial function was assessed by peak strain and strain rate. End-diastole was defined at the peak R of the electrocardiographic QRS-complex, end-systole at aortic valve closure as determined in the apical long-axis view. Timing of end-systole was then automatically transferred to images from the other projections, adjusted for cycle length. The endocardial border was drawn manually and the thickness of the region of interest adjusted to cover the myocardium but exclude the pericardium. Automated tracking was performed, visually evaluated and, if necessary, manually corrected.

Longitudinal regional function was measured in the entire LV subdivided into 6 wall regions and in the RV free wall, each wall region automatically further subdivided into three segments (apical, mid and basal) by the software. Circumferential regional function was measured in the LV at the apical, mid and basal ventricular level. Each slice was automatically subdivided in six equiangular segments corresponding to the ventricular wall regions analyzed for longitudinal function (Figure 7). Due to inadequate image quality, speckle tracking could not be performed on short-axis sections of the RV. Circumferential shortening in the mid segment of the RV free wall was therefore assessed by TDI. Longitudinal and circumferential peak systolic strain and strain rate for all segments were obtained and averaged to express global LV longitudinal and circumferential strain and strain rate. Ventricular rotation was assessed in the apical and basal short-axis view of the LV. End-systolic rotation was measured in the six equiangular segments and rotation for each slice calculated. Clockwise rotation, as viewed from the apex, was defined as positive, while counter-clockwise rotation was defined as negative. Ventricular torsion was then calculated as the difference between basal and apical rotation.

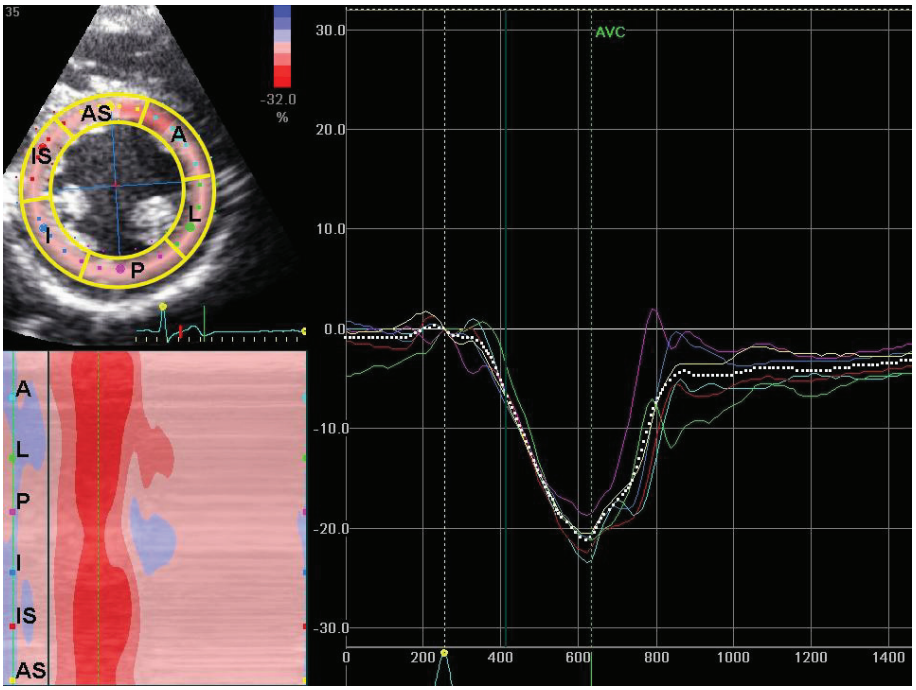

Figure 7

Speckle tracking echocardiography. In the upper left hand panel, a short-axis section of the left ventricle with schematic illustration of how endo- and epicardial borders were defined and the slice then divided into 6 equiangular segments (corresponding to the ventricular walls used in standard analyses of regional wall motion). In the lower left hand panel, a color-coded M-mode recording is shown. In the right hand panel, the strain curves from the respective segments are shown, with the white dotted line representing the average circumferential strain. A, anterior wall; AS, anterior septum; I, inferior wall; IS, inferior septum; L, lateral wall; P, posterior wall.

Statistical analysis

All data are presented as mean±SD. Statistical analysis was performed using SPSS 12.0.1 and GraphPad Prism version 4.00. Student's t-test was used for comparisons between two groups and one-way ANOVA with post-hoc Bonferroni correction for comparisons between more than two groups. Pearson's correlation coefficient was used where appropriate. Inter- and intraobserver variability were assessed by the intraclass correlation coefficient (α-value). TDI and MRI strain measurements were compared by a Bland-Altman plot. A value of $p<0.05$ was considered significant.

Summary of results

Paper 1

The contraction pattern of the systemic RV in 14 Senning-operated TGA patients was compared with findings in the RV and LV of normal subjects (n=14) and of patients successfully operated for congenital heart disease with a systemic LV (n=14). Ventricular contraction pattern was described in terms of longitudinal and circumferential shortening, assessed by TDI, and ventricular torsion, assessed by MRI.

Systemic RV EF by MRI was 47±8 %, RV EF in healthy controls was 54±5 % ($p=0.02$). Peak ventilatory oxygen uptake in the Senning-patients was 65±11% of the expected value.

In the Senning-operated patients there was a leftward shift of the IVS, manifested as a higher ratio between the RV and LV diameter than in normal subjects (1.28±0.32 vs. 0.54±0.10, $p<0.001$). The radius of curvature of the systemic RV free wall was less than that of the normal RV (2.11±0.39 cm vs. 3.09±0.49 cm, $p<0.001$) but similar to that of the normal LV (2.11±0.39 cm vs. 2.37±0.29 cm, NS).

In the systemic RV free wall, circumferential strain exceeded longitudinal strain (-23.3±3.4% vs. -15.0±3.0%, $p<0.001$) as in the normal LV (-25.7±3.1% vs. -16.5±1.7%, $p<0.001$), but opposite to the findings in the normal RV (-15.8±1.3% vs. -30.7±3.3%, $p<0.001$). Strain in the IVS in the TGA patients did not differ from normal. Strain rate values in the systemic RV free wall and IVS of the Senning-operated patients were significantly less than in the normal LV and IVS. There was no significant difference in strain or strain rate between the operated controls and the healthy controls, neither for the RV nor the LV. There was good agreement between strain obtained by TDI and MRI.

In the normal LV, there was global clockwise rotation of the base of the ventricle and counter-clockwise rotation of the apex, 5.1±1.5° and -11.6±4.6°, respectively ($p<0.001$), with resulting torsion of 16.7 ± 4.8°. Similarly, the RV free wall in the normal heart rotated with the LV, with a resulting torsion of 11.4±2.6°. In contrast, global rotation of the systemic RV was essentially absent both at the basal and apical levels, 0.3±1.3° and 0.0±2.1°, respectively (NS). Consequently, there was no significant global torsion of the systemic RV (0.3±1.8°).

Key findings: In the systemic RV as in the normal LV, there was predominant circumferential over longitudinal free wall shortening, opposite to findings in the normal RV. However, the systemic RV did not display torsion as found in the normal LV.

Paper 2

The subpulmonary LV contraction pattern in 14 Senning-operated TGA patients was studied and described in terms of longitudinal and circumferential shortening, assessed by TDI, and ventricular torsion, assessed by MRI.

Subpulmonary LV EF was 53±11 %, LV EF in healthy controls was 59±7 % (NS). The radius of curvature of the subpulmonary LV free wall was greater than that of the normal LV (3.29±0.80 cm vs. 2.37±0.29 cm, $p<0.001$) but similar to the normal RV free wall radius of curvature (3.29±0.80 cm vs. 3.09±0.49 cm, NS).

In the subpulmonary LV free wall, longitudinal strain was greater than circumferential strain (-23.6±3.6% vs. -19.1±3.2%, $p=0.002$) as in the normal RV (-30.7±3.3% vs. -15.8±1.3%, $p<0.001$), but opposite to findings in the normal LV (-16.5±1.7% vs. -25.7±3.1%, $p<0.001$). However, subpulmonary strain and strain rate values were intermediate between those in the normal LV and RV.

Ventricular free wall torsion was reduced in the subpulmonary LV compared with both the normal LV (5.7±3.2° vs. 16.7±5.6°, $p<0.001$) and RV (5.7±3.2° vs. 11.4±2.6°, $p<0.05$).

Key findings: The subpulmonary LV displayed predominantly longitudinal shortening as did its physiological counterpart, the normal RV. However, the degree and rate of both longitudinal and circumferential shortening were intermediate between those of the LV and RV of the normal heart. Ventricular free wall torsion was reduced in the subpulmonary LV compared with both the normal LV and RV.

Paper 3

Ventricular function in 22 TGA patients operated with arterial switch and 22 healthy controls was studied. Myocardial deformation was described in terms of longitudinal and circumferential shortening and ventricular torsion, measured by STE. Strain values from all segments were averaged to obtain global longitudinal and circumferential strain.

Left ventricular EF was 56±4 % in controls and 57±5 % in patients (NS) and LV volumes and mass measured by MRI were not significantly different between the groups. Peak ventilatory oxygen uptake in patients was 82±14 % of the expected value.

Ventricular geometry, assessed as the ratio between LV and RV end-systolic diameters, was not significantly different between patients and controls (1.38±0.13 vs. 1.45±0.11, NS).

In the LV of both patients and controls, global circumferential strain was greater than global longitudinal strain (-26.0±2.5 % vs. -18.3±1.3 %, $p<0.001$ and -26.2±2.4 % vs. -20.4±1.6 %, $p<0.001$, respectively). In the TGA patients, global LV longitudinal strain was lower than in controls (-18.3±1.3 % vs. -20.4±1.6 %, $p<0.001$), while global longitudinal strain rate was similar (-1.21±0.13 s^{-1} vs. -1.27±0.12 s^{-1}, NS). Longitudinal strain was reduced in all ventricular regions except the posterior wall, most pronounced in the apical segments. LV circumferential shortening was similar in the two groups.

In the RV, longitudinal shortening was greater than circumferential shortening in both patients and controls (-28.7±4.0 % vs. -14.5±1.8 %, $p<0.0001$ and -31.9±5.3 % vs. -14.3±2.2 %, $p<0.0001$, values from the mid segment). RV longitudinal strain was slightly, but significantly, reduced at the mid-ventricular and apical level in patients, while there was no significant difference in RV circumferential strain between patients and controls.

Both basal and apical rotation were reduced in patients compared to controls, and the resulting torsion was less in patients than in controls (12.4±2.9º vs. 16.3±2.6º, $p<0.001$). While rotation was distributed relatively homogenously in the normal LV, there was greater dispersion of rotation in the LV of the TGA patients, with basal rotation being greatest in the inferior wall and apical rotation being greatest in the anterior wall.

Key findings: In the TGA patients, there was slightly reduced longitudinal shortening in both ventricles and reduced LV torsion, although standard measures of global ventricular function were normal.

Discussion

Senning-operated patients – permanently altered ventricular roles

Systemic right ventricle

In the Senning-operated patients, we found a strain pattern in the free wall of the systemic RV with predominant circumferential over longitudinal shortening, similar to that found in the normal LV and opposite to that found in the normal RV (Figure 8). Strain rate, however, was significantly decreased in the systemic RV compared with the normal LV, and ventricular torsion was absent (Figure 9).

Adaptive changes or myocardial dysfunction?

The first question that will be addressed is whether these changes in the systemic RV are the result of a physiological adaptation to the increased load or represent impaired myocardial function. None of the patients had clinical evidence of heart failure, and the mean systemic RV EF was close to that reported as normal in this setting (30). Furthermore, the strain pattern and values in the systemic RV were not significantly different from those found in the normal LV. Moreover, the contraction pattern was uniform in all patients with systemic RV, regardless of their RV EF. These findings suggest that the predominance of circumferential over longitudinal shortening in the RV of the Senning-operated patients is an adaptive response to the systemic workload.

A possible explanation for this contraction pattern might be the altered geometry of the systemic RV. In the Senning-operated patients, there is a leftward shift of the IVS resulting in a more circular shape of the systemic RV, reflected by an increased ratio between RV and LV diameter. There is also a decreased RV free wall radius of curvature. This renders the systemic RV more similar to the normal LV in a short-axis section. In addition, in the setting of RV pressure overload it is mainly the middle circumferential layer that hypertrophies (31, 32), making the RV also in this respect more like the normal LV, which has a well-developed circumferential layer (33). These changes might facilitate circumferential shortening through alterations in regional wall stress.

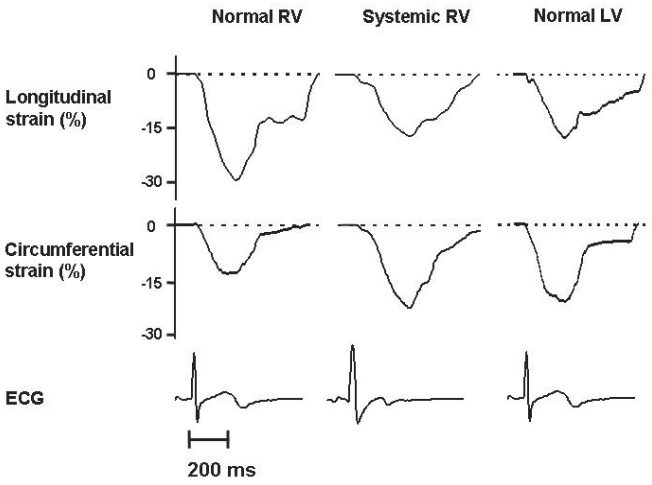

Figure 8

Representative strain recordings from the systemic right ventricle (RV), the normal left ventricle (LV) and normal RV. The systemic RV displays a shortening pattern similar to that found in the normal LV with predominant circumferential over longitudinal shortening, opposite to the pattern found in the normal RV.

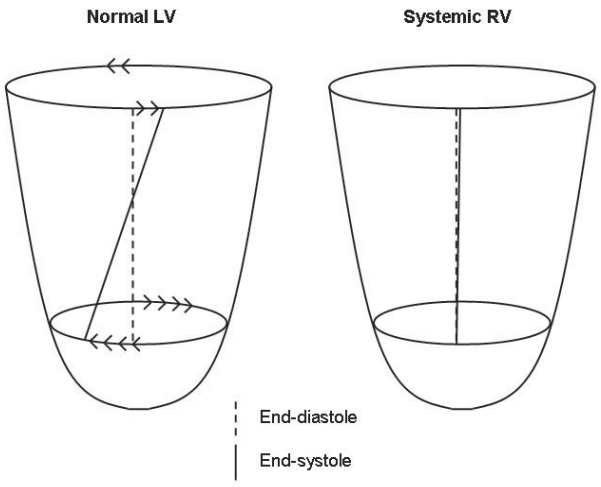

Figure 9

Schematic drawing of ventricular torsion. In the normal left ventricle (LV), the apex rotates counter-clockwise in systole (viewed from the apex) and the base clockwise, creating ventricular torsion. In the systemic right ventricle (RV), there was essentially no rotation of apex or base and thus no ventricular torsion.

Another possible explanation is that there exist congenital differences in fibre architecture between normal hearts and the hearts of patients with TGA accounting for the respective contraction patterns. This issue will be addressed below, in the integrated discussion of ventricular physiology.

Sterno- and pericardiotomy as a cause of the systemic RV contraction pattern should also be considered. This hypothesis is less probable, as we did not find an altered RV contraction pattern in the control group consisting of operated patients with a systemic LV. Furthermore, deformation variables have been studied under open-heart surgery, demonstrating that strain and strain rate are not affected by sterno- or pericardiotomy, while tissue velocities are significantly altered during the operative procedure (34, 35).

While strain values were similar between the systemic RV and normal LV, *strain rate* values in the systemic RV, however, were decreased compared to the normal LV. This could indicate incipient myocardial dysfunction, as strain rate has been reported to be a more sensitive measure of intrinsic myocardial function (36, 37). Another finding suggesting possible myocardial dysfunction is the absence of ventricular torsion in the systemic RV. As ventricular torsion may contribute to energy-efficient ejection (38), the lack thereof could represent a potential for future myocardial failure. Reduced ventricular torsion has been reported in a number of heart diseases (39-41).

Possible causes of incipient myocardial dysfunction

Systemic RV failure, along with arrhythmia, is a primary concern in the follow-up of this patient group. The etiology of myocardial dysfunction is most likely multifactorial: ischemia, inappropriate hypertrophy due to increased load or valvular pathology might all contribute to its development.

The risks of ischemic damage to the systemic RV are many: the operation itself, which involves circulatory arrest, coronary anomalies (42), as well as documented dynamic myocardial perfusion defects (43, 44), making the RV more sensitive to cardiac stress. Ideally, our measurements of regional deformation variables should be correlated to angiographic findings; however, this was not clinically indicated and thus precluded for ethical reasons.

Myocardial hypertrophy may be inappropriate, and combined with inadequate perfusion, may constitute a potential for development of myocardial fibrosis and depressed function. Late gadolinium enhancement by MRI, suggestive of myocardial fibrosis, has been documented in a significant proportion of patients with a systemic RV and found to correlate with adverse outcome (45, 46).

Tricuspid regurgitation might also constitute a factor in the progression towards systemic RV failure; however, in the present study, tricuspid regurgitation was of possible hemodynamic significance only in three patients.

Some special considerations in addition to the abovementioned factors apply to the finding of reduced ventricular torsion. In the RV, pressure overload leads to preferential hypertrophy of the circumferential fibres, while the fraction of obliquely oriented fibres is reduced compared to the normal RV (32). Since contraction of the obliquely oriented fibres are responsible for ventricular torsion, a reduction in their relative share of the total myocardial mass might lead to a reduction in torsion. The absence of torsion could also be the result of increased afterload, mediated through changes in wall stress (47).

Subpulmonary left ventricle

In the subpulmonary LV, there was predominant longitudinal over circumferential shortening in the free wall, as in the normal RV. However, the degree and rate of both longitudinal and circumferential shortening were intermediate between those of the normal LV and RV. Subpulmonary LV free wall torsion was less than in both the LV and RV of the normal heart.

These findings indicate that the shortening pattern reflects the role of the LV as the subpulmonary ventricle, but also only a partial adaptation to the decreased load. The factors discussed above as influencing the contraction pattern of the systemic RV can also be applied to the subpulmonary LV, with some modifications.

There is an increased radius of curvature as well as the previously described septal shift, thus rendering the subpulmonary LV similar to the normal RV in the short-axis section. The demonstrated contraction pattern might reflect changes in regional wall stress resulting from these alterations in ventricular geometry. Ventricular mass, however, was not significantly different between the normal LV and the subpulmonary LV. This could suggest

that myocardial structure is relatively well preserved in the subpulmonary LV, which may partly explain why the strain values of the subpulmonary LV remain intermediate between those of the normal LV and RV.

The strain rate values in the subpulmonary LV are also intermediate between those in the normal LV and RV. While the systemic RV displayed strain values similar to those of the normal LV, but reduced strain rate values, there was no such dissociation between strain and strain rate in the subpulmonary LV. With regard to strain rate, there is therefore no clear indication of reduced myocardial function in the subpulmonary LV.

Reduced ventricular torsion could be a marker of incipient myocardial dysfunction, although there are other possible explanations for this finding. The reduction in torsion in the subpulmonary LV might be the result of absent torsion in the systemic RV. In the normal heart, the RV twists with the LV (48), and torsion of the subpulmonary ventricle may at least partially depend on torsion of the systemic ventricle, or the ventricle that is dominant in terms of mass, by ventricular interaction. The leftward septal shift might also play a role in the reduction of subpulmonary LV torsion.

Arterial switch-operated patients – normalized ventricular roles

Global ventricular function, dimensions and overall geometry were similar in the arterial switch-operated patients and healthy controls. However, SDE disclosed changes in myocardial deformation that were not apparent using traditional measures of ventricular function. In the LV of patients operated with arterial switch, global longitudinal strain was reduced compared to healthy controls, while circumferential strain was not significantly different between the two groups. There was no difference in strain rate between the groups. Ventricular torsion was reduced in patients, and patients showed greater regional dispersion of rotation.

Possible reasons for the reduction in global longitudinal strain and reduced ventricular torsion are similar to the ones discussed above regarding the Senning-operated patients, principally ischemic myocardial damage, as well as alterations in ventricular geometry inherent in the malformation. Patients operated with arterial switch are perhaps particularly at risk of intraoperative ischemic damage, as the operation involves reimplantation of the coronary arteries. Coronary occlusion and stenoses are also recognized post-operative

complications (11). Coronary anomalies, particularly a hypoplastic LAD (49) may also contribute to longitudinal shortening being most reduced in the apical segments. Reduced coronary flow reserve (50) and wall motion abnormalities during stress as well as reversible myocardial perfusion defects have been documented in this patient group (51).

The longitudinal fibres are located predominantly in the subendocardial layer, and are therefore probably particularly susceptible to ischemic damage. Early myocardial dysfunction would thus first become manifest as a reduction in longitudinal shortening, which has been demonstrated in a number of cardiac diseases (52, 53). Suggesting that our findings might represent incipient myocardial dysfunction is the recent report of reduced global ventricular function in arterial switch-operated patients at 16-year follow-up (54). Our patients were younger, and global ventricular failure might not yet be apparent.

Somewhat surprisingly, strain rate was not significantly reduced in the patient group, although there was a trend towards lower values than in the healthy controls ($p=0.12$). There is, however, greater variability in the strain rate measurements, which, along with a relatively small number of patients could result in lack of statistical significance.

Alterations in ventricular geometry inherent in the malformation are a less likely explanation for the depressed longitudinal function, as the decreased shortening was more pronounced at the apical level. If inherent structural abnormalities were responsible, one would expect the greatest reduction in function to be located at the basal level in relation to the outlets of the great arteries (55). Structural differences in myocardial architecture might, however, contribute to the greater regional dispersion of rotation with rotation being most reduced in the anterior and anterior septal segments of the basal plane, which is the location of the outlet tract.

Integrated discussion of ventricular physiology and clinical significance

In summary, the systemic RV in Senning-operated patients displays a geometry and strain pattern similar to the normal LV, as does the LV in arterial switch-operated patients. The similarity between the normal LV and the LV of arterial switch-operated patients renders less likely the hypothesis that congenital differences in ventricular architecture are the cause of the observed contraction patterns in the TGA patients. The strain pattern of the systemic ventricle in TGA patients, whether it be the RV in Senning-operated or the LV in arterial switch-operated patients, consequently seems to be mainly the result of loading conditions mediated through overall ventricular geometry rather than congenital differences in ventricular architecture.

Systemic ventricular function is considered adequate in both patients groups, as both the Senning- and arterial switch-operated patients were asymptomatic and none showed signs of congestive heart failure. Symptoms can be underreported, though, especially in patients with congential heart disease perhaps accustomed to a lower activity level.

However, the congenital malformation in itself with its associated perfusion anomalies, the operative procedure and, in the case of the systemic RV, the sustained increased load on a ventricle designed for a low-pressure circulation, most likely take their toll on ventricular function. The demonstrated reductions in myocardial deformation probably do indicate some degree of myocardial pathology.

Supporting the assumption of myocardial dysfunction is the finding of reduced exercise peak ventilatory oxygen uptake in both atrial- and arterial-switch operated patients, most pronounced in the Senning group. These findings are in keeping with those of other studies (56-59). The diminished exercise capacity does not, however, unequivocally indicate ventricular failure. For the Senning-operated patients, failure to increase atrioventricular filling rates during exercise might also play a part (60). Alterations in pulmonary function might also be responsible for the depressed peak oxygen uptake, demonstrated in patients after surgery for a number of congenital heart conditions (61, 62).

Incipient ventricular dysfunction seems to be more advanced in the systemic RV than in the LV of the arterial switch-operated patients. Significantly reduced EF, total absence of torsion and depressed strain rate compared to the normal LV signify a more severe dysfunction than a relatively small reduction in longitudinal strain and ventricular torsion.

This suggests that the RV is perhaps less suited over time to carry the systemic load. However, the Senning-operated patients were older and the follow-up period thus longer in this patient group.

Ventricular geometry and strain values in the IVS of Senning-operated patients suggest that the IVS functions as a part of the systemic ventricle and not the anatomical LV. The IVS is displaced towards the LV cavity, and strain values are similar to those in the normal LV and systemic RV free wall. If the IVS remained a functional part of the subpulmonary LV, one would expect an increase in longitudinal strain in the IVS relative to the normal LV similar to that found in the subpulmonary LV free wall.

Our findings suggest that analysis of deformation variables may provide useful information both concerning ventricular physiology and clinical follow-up of this patient group. In the Senning-operated patients, a strain pattern most likely the result of an adaption to alterations in load was detected. In the case of the arterial-switch operated patients, standard measures of global ventricular function did not disclose reduced function, while deformation variables detected both subtle global and regional changes in myocardial contraction.

Methodological issues

Patient and control group selection

Patients were identified from operation records at Oslo University Hospital Rikshospitalet. Patients without associated hemodynamically significant lesions were selected. Those unable to perform exercise testing due to physical or mental disability were not included. The selected Senning-patients were operated over a 4-year period (1984-1987), the arterial switch-patients over a 9-year period (1989-1997). Improvement in operator technique and experience might reduce per- and postoperative complications, including ischemic damage to the myocardium. However, this should not have any bearing on the main findings concerning the ventricular shortening pattern, i.e. the balance between longitudinal and circumferential contraction. Operator technique might be of importance with regard to the findings suggesting decreased myocardial function, though, as duration of ischemia could be a determinant of subsequent dysfunction. However, no correlation was found in the arterial switch-group between strain values and time on extracorporeal circulation or aortic cross-

clamp time. Furthermore, our study groups were too small to study the effect of a possible development in surgical technique on the relevant deformation variables.

Our study results are limited to asymptomatic patients with adequate systemic ventricular function, as no patients with signs of overt heart failure were included. Further studies are needed to elucidate how the contraction pattern changes with the development of manifest heart failure.

In order to evaluate whether the observed contraction pattern in the systemic RV could be merely a post-operative effect, we included a control group in paper 1 consisting of patients who had undergone cardiac surgery but with normal ventricular roles, i.e. a systemic LV. We could not exclude that the underlying condition that dictated surgery affected ventricular function, but the objective was to assess the main features of the contraction pattern, i.e. the balance between longitudinal and circumferential contraction more than absolute values. The ideal control group does not exist, as it would consist of subjects without cardiac pathology undergoing a sham operation, which of course is precluded.

The control group included, among other patient groups, 6 patients operated with arterial switch for TGA, subjects that were part of the patient group in paper 3. While we found no difference in paper 1 between healthy controls and the operated control group, in paper 3 we did find a significant difference in longitudinal strain between healthy volunteers and the patients. This is most likely due to the relatively small changes in LV function documented in paper 3 being masked by the values from the other patients in the control group in paper 1 and therefore not statistically significant. Again, however, the main objective in paper 1 was to compare contraction *patterns* rather than absolute values.

Subjects in the healthy control group in paper 1 were slightly older than the patients. It is, however, unlikely that this small difference in age should account for our findings, as RV longitudinal function decreases with age (63), and we found greater RV longitudinal contraction in the control group than in the patients.

Assessment of myocardial deformation

Tissue Doppler and speckle tracking imaging are established and validated techniques for quantifying regional myocardial function (20, 21, 25, 26). Both techniques theoretically permit measurement of deformation in three dimensions: longitudinal, circumferential and

radial shortening or thickening. With TDI, however, circumferential and radial deformation can only be assessed in certain segments due to angle dependency. In the present studies, strain and strain rate were assessed only in two dimensions: longitudinal and circumferential. Radial strain was not measured and might have added additional information. We found it difficult to utilize radial strain, primarily because of tracking failure and therefore high variability of the measurements. A further limitation is that in the RV, circumferential strain could only be assessed by TDI due to image quality and thus only in the free wall.

Tissue Doppler imaging

As previously mentioned, the technique is dependent on angle of insonation relative to the direction of myocardial shortening and frame rate. Care was taken to align the ultrasound beam with the wall region where the sample volume was placed. Sector width was narrowed to obtain the highest frame rate possible. In paper 1, frame rate was 90-240 frames/second, which we consider sufficient to provide peak values both for strain and strain rate.

There is also a tendency for the strain curve to drift throughout the cardiac cycle. This is corrected for by forcing the strain curve to return to zero at end-diastole by linear compensation, which assumes that drift is equally distributed throughout the cardiac cycle. This is not necessarily correct, as drifting may be more pronounced in cardiac phases with rapid deformation.

Another problem with TDI is the repeatability of sample volume placement. In order to minimize error from different sample volume placement in different subjects, the region of interest was placed in the basal third of the apical and mid ventricular segments and in the middle of the basal segment (to avoid the mitral ring) in the standard apical projections for measurement of longitudinal function. For measurement of circumferential function, the papillary muscles were used to localize the mid-ventricular level and the region of interest placed in the free wall where the beam was tangential to the ventricular short-axis section.

There are also possible influences on measurements from the physiological state of the examined subject. Tissue Doppler recordings were obtained at the end of the echocardiographic examination when the subject would be expected to be in a resting state. Beat-to-beat variation in stroke volume might also affect strain measurements, and in order to minimize biological variability, all TDI measurements were averaged over 3 cardiac cycles.

In spite of several possible sources of error, TDI measurements showed good agreement with values obtained by analysis of tagged MRI images.

Speckle tracking echocardiography

Speckle tracking echocardiography has the advantage of not being angle-dependent. There is also less of a problem with sample volume placement, as long as standard echocardiographic projections are used.

However, since gray scale images are used and sector width cannot be narrowed beyond a full ventricular image, it might be difficult to obtain a sufficient frame rate. In paper 3, frames rates were 69-112 frames/second. This is within the interval generally agreed on as sufficient for analysis of strain and strain rate. However, some deformation variables, especially peak strain rate values, may still be underestimated, and we found lower peak systolic strain rate values in healthy controls in paper 3, using STE, than in paper 1, using TDI.

Image quality is also of paramount importance. Care was taken to adjust transducer frequency, sector width and focus depth to optimize the quality of the images.

There are also certain limitations pertaining to short-axis imaging, primarily out-of-plane movement due to cardiac translation and longitudinal shortening. This problem is greater at the base, since the mitral plane moves towards the apex in systole. Another possible cause of error is the problem of obtaining short-axis sections at the same levels in all patients. To minimize the variability introduced by this factor, we used anatomical landmarks when orienting the images – the mitral plane at the basal level and the most distal plane not showing systolic luminal closure at the apical level.

Despite these factors, intra- and interobserver variability was within acceptable limits. For each patient, several loops consisting of three cycles were recorded in each standard echocardiographic projection. When investigating interobserver variability, choice of loop was at the observer's discretion; accordingly, analysis of interobserver variability was not necessarily performed on the same loop by the two observers.

Global ventricular strain might prove a robust measure of ventricular function, less susceptible to the variability of individual strain measurements since it is an average of 18 segmental values. However, this might also make it less sensitive in picking up incipient

myocardial dysfunction, supposing that ventricular failure starts regionally and subsequently develops into a global condition. This assumption is supported by the finding of regional differences in strain reductions in the arterial switch-operated patients.

Magnetic resonance imaging

Apart from measurement of ventricular mass and volumes, MRI was used in paper I to validate circumferential strain measurements and to assess ventricular torsion.

Frame rate is a major limitation of this technique; a time resolution of 35 ms leaves a risk of underestimation of peak values. However, the strain curve does not have a sharp peak, but usually plateaus at peak shortening. Therefore, the risk of understimation of peak strain is less than for velocities and strain rate.

When comparing MRI and strain values, one must be sure that measurements are obtained at the same ventricular level. The same anatomical landmarks as for echocardiographic short-axis images were used.

Assessment of ventricular torsion

When measuring rotation in papers I and II, different centres of gravity were used for the systemic and subpulmonary ventricles. The reason for this is that the rotation algorithm in HARP presupposes a relatively circular short-axis shape. For the systemic ventricle, rotation of the entire ventricular slice could be calculated. However, the subpulmonary ventricle is more crescent-shaped in the short-axis section, and in order to assess rotation, we measured rotation of the entire heart using the common centre of gravity of the two ventricles as a reference point, subsequently extracting regional data for rotation of the free wall of the subpulmonary LV and normal RV. Thus, this is a source of error when comparing rotation and calculated torsion in the systemic and subpulmonary ventricles, but it should nonetheless be possible to compare direction and approximate magnitude of rotation.

When measuring rotation with STE, the same limitations apply as for strain in short-axis images, mainly frame rate, image quality, out-of-plane movement and variability in the placement of the short-axis sections.

Future perspectives

The findings in the present studies indicate further areas of research. From a pathophysiological viewpoint, studies are needed to clarify how the potential progression of ventricular dysfunction affects the myocardial contraction pattern. Furthermore, how is the contraction pattern affected in other conditions with RV pressure overload, such as pulmonary hypertension? Of clinical importance is whether – and if so, which - deformation variables can identify patients progressing to ventricular failure and therefore requiring closer follow-up and intervention.

Conclusions

1. Ventricular strain patterns in TGA patients seem to be mainly the result of loading conditions mediated through adaptive changes in ventricular geometry rather than alterations inherent in the congenital malformation.
    a. The systemic RV displays a short-axis geometry and strain pattern similar to the normal LV with predominant circumferential over longitudinal shortening, opposite to the pattern in the normal RV.
    b. In the subpulmonary LV, longitudinal contraction predominates over circumferential contraction, as in the normal RV, but absolute strain values are intermediate between the normal RV and LV, possibly indicating a partial adaption to the altered loading conditions.
    c. The LV of arterial switch-operated patients has the same overall contraction pattern as the normal LV, with predominant circumferential shortening.
2. Signs of incipient myocardial dysfunction are present in both atrial and arterial switch-operated patients, with more pronounced reductions in deformation variables in the atrial switch-operated group.
    a. In the systemic RV, strain rate is reduced and ventricular torsion absent compared to the normal LV.
    b. In the LV of arterial switch-operated patients, there is a slight reduction in global longitudinal strain and ventricular torsion compared to the normal LV.
3. Myocardial deformation analysis is of value in these patients, both in studying ventricular physiology and in assessing possible ventricular dysfunction not disclosed by standard measures of ventricular function.

Reference List

1. Hornung TS. Transposition of the Great Arteries. In: Gatzoulis MA, Webb G, Daubeney PEF, editors. Diagnosis and Management of Adult Congenital Heart Disease. Churchill Livingstone, 2003:349-62.

2. Senning A. Surgical correction of transposition of the great vessels. Surgery 1959; 45:966-80.

3. Mustard W. Successful Two-Stage Correction of Transposition of the Great Vessels. Surgery 1964; 55:469-72.

4. Oechslin E, Jenni R. 40 years after the first atrial switch procedure in patients with transposition of the great arteries: long-term results in Toronto and Zurich. Thorac Cardiovasc Surg 2000; 48:233-7.

5. Turina MI, Siebenmann R, von Segesser L, Schonbeck M, Senning A. Late functional deterioration after atrial correction for transposition of the great arteries. Circulation 1989; 80:I162-I167.

6. Gelatt M, Hamilton RM, McCrindle BW, Connelly M, Davis A, Harris L, Gow RM, Williams WG, Trusler GA, Freedom RM. Arrhythmia and mortality after the Mustard procedure: a 30-year single-center experience. J Am Coll Cardiol 1997; 29:194-201.

7. Wilson NJ, Clarkson PM, Barratt-Boyes BG, Calder AL, Whitlock RM, Easthope RN, Neutze JM. Long-term outcome after the Mustard repair for simple transposition of the great arteries. 28-year follow-up. J Am Coll Cardiol 1998; 32:758-65.

8. Jatene AD, Fontes VF, Paulista PP, Souza LC, Neger F, Galantier M, Sousa JE. Anatomic correction of transposition of the great vessels. J Thorac Cardiovasc Surg 1976; 72:364-70.

9. Lecompte Y, Zannini L, Hazan E, Jarreau MM, Bex JP, Tu TV, Neveux JY. Anatomic correction of transposition of the great arteries. J Thorac Cardiovasc Surg 1981; 82:629-31.

10. Di Donato RM, Wernovsky G, Walsh EP, Colan SD, Lang P, Wessel DL, Jonas RA, Mayer JE, Jr., Castaneda AR. Results of the arterial switch operation for transposition of the great arteries with ventricular septal defect. Surgical considerations and midterm follow-up data. Circulation 1989; 80:1689-705.

11. Wernovsky G, Hougen TJ, Walsh EP, Sholler GF, Colan SD, Sanders SP, Parness IA, Keane JF, Mayer JE, Jonas RA, . Midterm results after the arterial switch operation for transposition of the great arteries with intact ventricular septum: clinical, hemodynamic, echocardiographic, and electrophysiologic data. Circulation 1988; 77:1333-44.

12. Marino BS, Wernovsky G, McElhinney DB, Jawad A, Kreb DL, Mantel SF, van der Woerd WL, Robbers-Visser D, Novello R, Gaynor JW, Spray TL, Cohen MS. Neo-aortic valvar function after the arterial switch. Cardiol Young 2006; 16:481-9.

13. Losay J, Touchot A, Serraf A, Litvinova A, Lambert V, Piot JD, Lacour-Gayet F, Capderou A, Planche C. Late outcome after arterial switch operation for transposition of the great arteries. Circulation 2001; 104:I121-I126.

14. von Bernuth G. 25 years after the first arterial switch procedure: mid-term results. Thorac Cardiovasc Surg 2000; 48:228-32.

15. Derrick GP, Josen M, Vogel M, Henein MY, Shinebourne EA, Redington AN. Abnormalities of right ventricular long axis function after atrial repair of transposition of the great arteries. Heart 2001; 86:203-6.

16. Eyskens B, Weidemann F, Kowalski M, Bogaert J, Dymarkowski S, Bijnens B, Gewillig M, Sutherland G, Mertens L. Regional right and left ventricular function after the Senning operation: an ultrasonic study of strain rate and strain. Cardiol Young 2004; 14:255-64.

17. Fredriksen PM, Ingjer F, Nystad W, Thaulow E. Aerobic testing of children and adolescents - a comparison of two treadmill-protocols. Scand J Med Sci Sports 1998; 8:203-7.

18. Hudsmith LE, Petersen SE, Francis JM, Robson MD, Neubauer S. Normal human left and right ventricular and left atrial dimensions using steady state free precession magnetic resonance imaging. J Cardiovasc Magn Reson 2005; 7:775-82.

19. Heimdal A, Stoylen A, Torp H, Skjaerpe T. Real-time strain rate imaging of the left ventricle by ultrasound. J Am Soc Echocardiogr 1998; 11:1013-9.

20. Urheim S, Edvardsen T, Torp H, Angelsen B, Smiseth OA. Myocardial strain by Doppler echocardiography. Validation of a new method to quantify regional myocardial function. Circulation 2000; 102:1158-64.

21. Edvardsen T, Gerber BL, Garot J, Bluemke DA, Lima JA, Smiseth OA. Quantitative assessment of intrinsic regional myocardial deformation by Doppler strain rate echocardiography in humans: validation against three-dimensional tagged magnetic resonance imaging. Circulation 2002; 106:50-6.

22. Skulstad H, Urheim S, Edvardsen T, Andersen K, Lyseggen E, Vartdal T, Ihlen H, Smiseth OA. Grading of myocardial dysfunction by tissue Doppler echocardiography: a comparison between velocity, displacement, and strain imaging in acute ischemia. J Am Coll Cardiol 2006; 47:1672-82.

23. Bohs LN, Trahey GE. A novel method for angle independent ultrasonic imaging of blood flow and tissue motion. IEEE Trans Biomed Eng 1991; 38:280-6.

24. Langeland S, D'Hooge J, Wouters PF, Leather HA, Claus P, Bijnens B, Sutherland GR. Experimental validation of a new ultrasound method for the simultaneous assessment of radial and longitudinal myocardial deformation independent of insonation angle. Circulation 2005; 112:2157-62.

25. Amundsen BH, Helle-Valle T, Edvardsen T, Torp H, Crosby J, Lyseggen E, Stoylen A, Ihlen H, Lima JA, Smiseth OA, Slordahl SA. Noninvasive myocardial strain measurement by speckle tracking echocardiography: validation against sonomicrometry and tagged magnetic resonance imaging. J Am Coll Cardiol 2006; 47:789-93.

26. Helle-Valle T, Crosby J, Edvardsen T, Lyseggen E, Amundsen BH, Smith HJ, Rosen BD, Lima JA, Torp H, Ihlen H, Smiseth OA. New noninvasive method for assessment of left ventricular rotation: speckle tracking echocardiography. Circulation 2005; 112:3149-56.

27. Lima JA, Jeremy R, Guier W, Bouton S, Zerhouni EA, McVeigh E, Buchalter MB, Weisfeldt ML, Shapiro EP, Weiss JL. Accurate systolic wall thickening by nuclear magnetic resonance imaging with tissue tagging: correlation with sonomicrometers in normal and ischemic myocardium. J Am Coll Cardiol 1993; 21:1741-51.

28. Moore CC, O'Dell WG, McVeigh ER, Zerhouni EA. Calculation of three-dimensional left ventricular strains from biplanar tagged MR images. J Magn Reson Imaging 1992; 2:165-75.

29. Garot J, Bluemke DA, Osman NF, Rochitte CE, McVeigh ER, Zerhouni EA, Prince JL, Lima JA. Fast determination of regional myocardial strain fields from tagged cardiac images using harmonic phase MRI. Circulation 2000; 101:981-8.

30. Hornung TS, Derrick GP, Deanfield JE, Redington AN. Transposition complexes in the adult: a changing perspective. Cardiol Clin 2002; 20:405-20.

31. Sanchez-Quintana D, Anderson RH, Ho SY. Ventricular myoarchitecture in tetralogy of Fallot. Heart 1996; 76:280-6.

32. Tezuka F, Hort W, Lange PE, Nurnberg JH. Muscle fiber orientation in the development and regression of right ventricular hypertrophy in pigs. Acta Pathol Jpn 1990; 40:402-7.

33. Greenbaum RA, Ho SY, Gibson DG, Becker AE, Anderson RH. Left ventricular fibre architecture in man. Br Heart J 1981; 45:248-63.

34. Skulstad H, Andersen K, Edvardsen T, Rein KA, Tønnessen TI, Hol PK, Fosse E, Ihlen H. Detection of ischemia and new insight into left ventricular physiology by strain Doppler and tissue velocity imaging: assessment during coronary bypass operation of the beating heart. J Am Soc Echocardiogr 2004; 17:1225-33.

35. Simmons LA, Weidemann F, Sutherland GR, D'Hooge J, Bijnens B, Sergeant P, Wouters PF. Doppler tissue velocity, strain, and strain rate imaging with transesophageal echocardiography in the operating room: a feasibility study. J Am Soc Echocardiogr 2002; 15:768-76.

36. Weidemann F, Jamal F, Sutherland GR, Claus P, Kowalski M, Hatle L, De S, I, Bijnens B, Rademakers FE. Myocardial function defined by strain rate and strain during alterations in inotropic states and heart rate. Am J Physiol Heart Circ Physiol 2002; 283:H792-H799.

37. Greenberg NL, Firstenberg MS, Castro PL, Main M, Travaglini A, Odabashian JA, Drinko JK, Rodriguez LL, Thomas JD, Garcia MJ. Doppler-derived myocardial systolic strain rate is a strong index of left ventricular contractility. Circulation 2002; 105:99-105.

38. Beyar R, Sideman S. Left ventricular mechanics related to the local distribution of oxygen demand throughout the wall. Circ Res 1986; 58:664-77.

39. Fuchs E, Muller MF, Oswald H, Thony H, Mohacsi P, Hess OM. Cardiac rotation and relaxation in patients with chronic heart failure. Eur J Heart Fail 2004; 6:715-22.

40. Tibayan FA, Rodriguez F, Langer F, Zasio MK, Bailey L, Liang D, Daughters GT, Ingels NB, Jr., Miller DC. Alterations in left ventricular torsion and diastolic recoil after myocardial infarction with and without chronic ischemic mitral regurgitation. Circulation 2004; 110:II109-II114.

41. Chang SA, Kim HK, Kim DH, Kim YJ, Sohn DW, Oh BH, Park YB. Left ventricular twist mechanics in patients with apical hypertrophic cardiomyopathy. Heart 2009.

42. Smith A, Arnold R, Wilkinson JL, Hamilton DI, McKay R, Anderson RH. An anatomical study of the patterns of the coronary arteries and sinus nodal artery in complete transposition. Int J Cardiol 1986; 12:295-307.

43. Lubiszewska B, Gosiewska E, Hoffman P, Teresinska A, Rozanski J, Piotrowski W, Rydlewska-Sadowska W, Kubicka K, Ruzyllo W. Myocardial perfusion and function of

the systemic right ventricle in patients after atrial switch procedure for complete transposition: long-term follow-up. J Am Coll Cardiol 2000; 36:1365-70.

44. Millane T, Bernard EJ, Jaeggi E, Howman-Giles RB, Uren RF, Cartmill TB, Hawker RE, Celermajer DS. Role of ischemia and infarction in late right ventricular dysfunction after atrial repair of transposition of the great arteries. J Am Coll Cardiol 2000; 35:1661-8.

45. Babu-Narayan SV, Goktekin O, Moon JC, Broberg CS, Pantely GA, Pennell DJ, Gatzoulis MA, Kilner PJ. Late gadolinium enhancement cardiovascular magnetic resonance of the systemic right ventricle in adults with previous atrial redirection surgery for transposition of the great arteries. Circulation 2005; 111:2091-8.

46. Giardini A, Lovato L, Donti A, Formigari R, Oppido G, Gargiulo G, Picchio FM, Fattori R. Relation between right ventricular structural alterations and markers of adverse clinical outcome in adults with systemic right ventricle and either congenital complete (after Senning operation) or congenitally corrected transposition of the great arteries. Am J Cardiol 2006; 98:1277-82.

47. Carasso S, Cohen O, Mutlak D, Adler Z, Lessick J, Reisner SA, Rakowski H, Bolotin G, Agmon Y. Differential effects of afterload on left ventricular long- and short-axis function: insights from a clinical model of patients with aortic valve stenosis undergoing aortic valve replacement. Am Heart J 2009; 158:540-5.

48. Haber I, Metaxas DN, Geva T, Axel L. Three-dimensional systolic kinematics of the right ventricle. Am J Physiol Heart Circ Physiol 2005; 289:H1826-H1833.

49. Hauser M, Bengel FM, Kuhn A, Sauer U, Zylla S, Braun SL, Nekolla SG, Oberhoffer R, Lange R, Schwaiger M, Hess J. Myocardial blood flow and flow reserve after

coronary reimplantation in patients after arterial switch and Ross operation. Circulation 2001; 103:1875-80.

50. Bengel FM, Hauser M, Duvernoy CS, Kuehn A, Ziegler SI, Stollfuss JC, Beckmann M, Sauer U, Muzik O, Schwaiger M, Hess J. Myocardial blood flow and coronary flow reserve late after anatomical correction of transposition of the great arteries. J Am Coll Cardiol 1998; 32:1955-61.

51. Hui L, Chau AK, Leung MP, Chiu CS, Cheung YF. Assessment of left ventricular function long term after arterial switch operation for transposition of the great arteries by dobutamine stress echocardiography. Heart 2005; 91:68-72.

52. Mogelvang R, Sogaard P, Pedersen SA, Olsen NT, Schnohr P, Jensen JS. Tissue Doppler echocardiography in persons with hypertension, diabetes, or ischaemic heart disease: the Copenhagen City Heart Study. Eur Heart J 2009; 30:731-9.

53. Nishikage T, Nakai H, Lang RM, Takeuchi M. Subclinical left ventricular longitudinal systolic dysfunction in hypertension with no evidence of heart failure. Circ J 2008; 72:189-94.

54. Grotenhuis HB, Ottenkamp J, Fontein D, Vliegen HW, Westenberg JJ, Kroft LJ, de Roos A. Aortic elasticity and left ventricular function after arterial switch operation: MR imaging--initial experience. Radiology 2008; 249:801-9.

55. Smith A, Wilkinson JL, Anderson RH, Arnold R, Dickinson DF. Architecture of the ventricular mass and atrioventricular valves in complete transposition with intact septum compared with the normal: I. The left ventricle, mitral valve, and interventricular septum. Pediatr Cardiol 1986; 6:253-7.

56. Douard H, Labbe L, Barat JL, Broustet JP, Baudet E, Choussat A. Cardiorespiratory response to exercise after venous switch operation for transposition of the great arteries. Chest 1997; 111:23-9.

57. Fredriksen PM, Pettersen E, Thaulow E. Declining aerobic capacity of patients with arterial and atrial switch procedures. Pediatr Cardiol 2009; 30:166-71.

58. Fredriksen PM, Ingjer F, Nystad W, Thaulow E. A comparison of VO_2(peak) between patients with congenital heart disease and healthy subjects, all aged 8-17 years. Eur J Appl Physiol Occup Physiol 1999; 80:409-16.

59. de Koning WB, Osch-Gevers M, Ten Harkel AD, van Domburg RT, Spijkerboer AW, Utens EM, Bogers AJ, Helbing WA. Follow-up outcomes 10 years after arterial switch operation for transposition of the great arteries: comparison of cardiological health status and health-related quality of life to those of the a normal reference population. Eur J Pediatr 2008; 167:995-1004.

60. Derrick GP, Narang I, White PA, Kelleher A, Bush A, Penny DJ, Redington AN. Failure of stroke volume augmentation during exercise and dobutamine stress is unrelated to load-independent indexes of right ventricular performance after the Mustard operation. Circulation 2000; 102:III154-III159.

61. Gilljam T, Sixt R. Lung function in relation to haemodynamic status after atrial redirection for transposition of the great arteries. Eur Heart J 1995; 16:1952-9.

62. Diller GP, Dimopoulos K, Okonko D, Li W, Babu-Narayan SV, Broberg CS, Johansson B, Bouzas B, Mullen MJ, Poole-Wilson PA, Francis DP, Gatzoulis MA. Exercise intolerance in adult congenital heart disease: comparative severity, correlates, and prognostic implication. Circulation 2005; 112:828-35.

63. Kukulski T, Hubbert L, Arnold M, Wranne B, Hatle L, Sutherland GR. Normal regional right ventricular function and its change with age: a Doppler myocardial imaging study. J Am Soc Echocardiogr 2000; 13:194-204.

Paper 1:

Pettersen E, Helle-Valle T, Edvardsen T, Lindberg H, Smith HJ, Smevik B, Smiseth OA, Andersen K. Contraction Pattern of the Systemic Right Ventricle - Shift from Longitudinal to Circumferential Shortening and Absent Global Ventricular Torsion. J Am Coll Cardiol. 2007; 49:2450-6.

Paper 2:

Pettersen E, Lindberg H, Smith HJ, Smevik B, Edvardsen T, Smiseth OA, Andersen K. Left Ventricular Function in Patients with Transposition of the Great Arteries Operated with Atrial Switch. Pediatr Cardiol. 2008; 29:597-603.

Paper 3:

Pettersen E, Fredriksen PM, Urheim S, Thaulow E, Smith HJ, Smevik B, Smiseth OA, Andersen K. Ventricular Function in Patients with Transposition of the Great Arteries Operated with Arterial Switch. Am J Cardiol. 2009; 104:583-9.

Erratum

p. 20 line 3: 'SR=(v(x)-v(x+Δx)/Δx' changed to 'SR=(v(x)-v(x+Δx))/Δx'